Rapid intercontinental air pollution transport associated with a meteorological bomb

A. Stohl, H. Huntrieser, A. Richter, S. Beirle, O. Cooper, S. Eckhardt, C. Forster, P. James, N. James, M. Wenig, et al.

Atmos. Chem. Phys. Discuss., 3, 2101–2141, 2003
www.atmos-chem-phys.org/acpd/3/2101/

Atmospheric Chemistry and Physics Discussions

Rapid intercontinental air pollution transport associated with a meteorological bomb

A. Stohl[1], H. Huntrieser[2], A. Richter[3], S. Beirle[4], O. Cooper[5], S. Eckhardt[1], C. Forster[1], P. James[1], N. Spichtinger[1], M. Wenig[6], T. Wagner[4], J. Burrows[3], and U. Platt[4]

[1]Department of Ecology, Technical University of Munich, Germany
[2]Institute for Atmospheric Physics, DLR, Oberpfaffenhofen, Germany
[3]Institute of Environmental Physics, University of Bremen, Germany
[4]Institute of Environmental Physics, Heidelberg University, Germany
[5]Cooperative Institute for Research in Environmental Sciences (CIRES), University of Colorado/NOAA Aeronomy Laboratory, Boulder, USA
[6]NASA Goddard Space Flight Center, Code 916, Greenbelt, MD, USA

Received: 19 February 2003 – Accepted: 1 April 2003 – Published: 16 April 2003

Correspondence to: A. Stohl (stohl@forst.tu-muenchen.de)

Abstract

Intercontinental transport (ICT) of trace substances normally occurs on timescales ranging from a few days to several weeks. In this paper an extraordinary episode in November 2001 is presented, where pollution transport across the North Atlantic took only about one day. The transport mechanism, termed here an intercontinental pollution express highway, was exceptional, as it involved an explosively generated cyclone, a so-called meteorological "bomb". To the authors' knowledge, this is the first study describing pollution transport in a bomb. The discovery of this event was based on transport model calculations and satellite measurements of NO_2, a species with a relatively short lifetime in the atmosphere, which could be transported that far only because of the high wind speeds produced by the bomb. A 15-year transport climatology shows that intercontinental express highways are about four times more frequent in winter than in summer, in agreement with bomb climatologies. The climatology furthermore reveals that intercontinental express highways may be important for the budget of short-lived substances in the remote troposphere. For instance, for a substance with a lifetime of 1 day, express highways may be responsible for about two thirds of the total ICT. A rough calculation suggests that express highways connecting North America with Europe enhance the average NO_x mixing ratios over Europe, due to North American emissions, by about 2–3 pptv in winter.

1. Introduction

1.1. Meteorological bombs

Cyclones are a key element of the atmospheric circulation in the midlatitudes (Carlson, 1998). Cyclogenesis, for which a first conceptual model was presented by the Bergen school (Bjerknes, 1910), occurs most frequently at the polar front. The various ascending and descending airstreams typically associated with these cyclones carry a range

ACPD

3, 2101–2141, 2003

of different chemical signatures (Cooper et al., 2002). The so-called warm conveyor belt (WCB) – a strongly ascending airstream ahead of a cyclone's cold front (Browning et al., 1973) – is an important mechanism to lift air pollutants emitted at the surface into the upper troposphere, where the faster winds facilitate their intercontinental transport (ICT) (Stohl and Trickl, 1999). Thus, cyclones are important not only for the dynamics of the atmosphere, but also for it's chemistry.

Some cyclones develop so explosively that they became known as meteorological "bombs" (Sanders and Gyakum, 1980). The characteristic features of a bomb are a rapid central pressure reduction and an attendant increase in intensity. Since the pioneering study of Sanders and Gyakum (1980), henceforth referred to as SG1980, explosive cyclogenesis is defined by a fall of more than $1\,\mathrm{hPa/h} \times (\sin\phi/\sin 60)$, where ϕ is latitude, of a cyclone's minimum sea-level pressure, over a period of at least 24 h.

Explosive cyclogenesis requires extremely high levels of baroclinicity near the cyclone track (Ulbrich et al., 2001) and/or extremely strong release of latent heat (Zhu and Newell 2000; Wernli et al. 2002). Cold air encircling the bomb's center at low altitudes pushes the warmer air up in a spiral-like way (Lemaître et al., 1999), which sometimes leads to eye-like structures known from tropical cyclones (SG1980). During their life-cycles, bombs can attain extremely low core sea-level pressures (SG1980), and, thus, horizontal pressure gradients – and surface winds – can be extreme. Their scales range from rather small-scale vortices that do not change the large-scale circulation significantly (Ulbrich et al., 2001) to larger-than-normal cyclones (Lim and Simmonds, 2002).

Bombs are a great danger, especially for shipping. For instance, the Sydney-Hobart yacht race cyclone in December 1998 resulted in the death of six race participants (Buckley and Leslie, 2000). Like tropical cyclones, bombs weaken after landfall, but to a much lesser extent. Surface wind gusts above $50\,\mathrm{m\,s^{-1}}$ have been reported over land. Examples of destructive bombs over Europe are the great storm of October 1987 over southern England (Burt and Mansfield, 1988) and the Christmas storms of 1999, that claimed 130 lives and caused 13 billion Euros worth of total economic

ACPD
3, 2101–2141, 2003

losses in central Europe (Ulbrich et al., 2001). The danger of bombs also comes from their explosive development and their rapid motion, both of which are often not well predicted by weather forecast models.

Explosive cyclogenesis is a phenomenon occurring most often in winter and almost exclusively over the oceans. About 50 bombs per year are found on the Northern Hemisphere (Lim and Simmonds, 2002), most of them over the warm surface waters downstream of Asia and North America (SG1980), regions with frequent and intense WCBs and corresponding strong latent heat release (Stohl, 2001). There is a statistically significant upward trend of global bomb occurrence during the last two decades, which may be related to global warming (Lim and Simmonds, 2002).

1.2. Long-range NO_x transport

ICT of trace substances is a topic that currently receives much attention, due to its implications both for air quality and climate. ICT is reasonably well documented (e.g. Jaffe et al. 1999; Stohl and Trickl 1999; Forster et al. 2001) for moderately long-lived species (e.g. carbon monoxide, ozone, aerosols), but so far has been considered insignificant for species with lifetimes of hours to a few days. Among these shorter-lived species, nitrogen oxides (NO_x) – which have a lifetime on the order of hours in the atmospheric boundary layer (ABL) and a few days in the upper troposphere (Jaeglé et al., 1998) – are of particular interest, because they are critical for photochemical formation of ozone (O_3) in the troposphere (Lin et al., 1988). Below a certain concentration of nitric oxide (NO), O_3 is destroyed, whereas above it is formed. Values of this so-called compensation point vary, but are on the order of 10 to 30 ppt, with lower values in the upper troposphere (e.g. Reeves et al., 2002). Aircraft measurements show that NO_x levels in the remote free troposphere, particularly in the upper troposphere, often exceed this threshold (Bradshaw et al., 2000), leading to substantial in-situ O_3 formation.

ICT of NO_x also can occur in the form of reservoir species (NO_y, e.g. peroxy acetyl nitrate), which are products from NO_x oxidation, from which NO_x can be re-cycled at a later time. This is thought to be important for photochemical O_3 formation in the

background free troposphere (e.g. Wild et al., 1996). However, even export of NO_y from the ABL to the free troposphere is very inefficient (Prados et al., 1999), with only about 5-10% of the originally emitted nitrogen remaining in the atmosphere after a few days (Stohl et al., 2002b), and only a small fraction of this being in the form of NO_x.

Given the inefficient vertical transport of boundary-layer NO_x, both aircraft (Ziereis et al., 2000) and, especially, lightning (Huntrieser et al. 2002; Jeker et al. 2000) emissions of NO_x are thought to play important roles in the free troposphere. Indeed, large-scale NO_x plumes have been found in the upper troposphere over North America (Brunner et al., 1998), that possibly were produced by lightning.

Satellite data from the Global Ozone Monitoring Experiment (GOME) (Burrows et al., 1999) confirm that, on a climatological basis, NO_x is highly concentrated in its major source regions, implying an average NO_x lifetime in the atmosphere of about 1 day (Leue et al., 2001). Nevertheless, two episodes where GOME showed ICT of NO_x were recently described. One was due to boreal forest fire emissions, where NO_x was injected directly into the free troposphere and subsequently transported rapidly from Canada to the west coast of Europe (Spichtinger et al., 2001). In the second case, NO_x from power plants in the South African Highveld, again injecting NO_x into the free troposphere, were transported to the Indian Ocean and, presumably, to Australia (Wenig et al., 2002). Furthermore, lightning NO_x emissions also played a role in this case.

In this paper, a third case of NO_x ICT is reported, that is, so far, the clearest example of its kind and does neither involve direct deposition of emissions into the free troposphere, nor significant lightning emissions. Instead, average advection speeds above $40\,m\,s^{-1}$ south of a bomb center allowed ICT of NO_x from anthropogenic surface sources to occur within less than two days. Furthermore, in order to judge the relevance of events similar to the one observed, a 15-year climatology of fast ICT of anthropogenic emission tracers is presented.

ACPD
3, 2101–2141, 2003

2. Methods

In November 2001, the first aircraft campaign of the CONTRACE (Convective Transport of Trace Gases into the Upper Troposphere over Europe: Budget and Impact on Chemistry) project took place in Germany. One aim of this project was to make measurements in the outflow of polluted North Atlantic WCBs. Due to successful tracer model forecasts (Lawrence et al. 2003; Stohl et al. 2003), it was indeed possible to probe pollution plumes from North America on three occasions, allowing, for the first time, a detailed chemical characterisation of such plumes over Europe (Huntrieser et al., 2003). After the campaign, tropospheric NO_2 columns retrieved from spectral data of the GOME satellite sensor (Burrows et al., 1999) were used as supplementary information on the transport of pollution plumes across the Atlantic. Unfortunately, few GOME data were available during the aircraft campaign, because the instrument was turned off for protection during the Leonides meteor shower. However, immediately before the first measurement flight, an episode of NO_2 transport from North America to Europe was seen in the GOME data, that agrees remarkably well with tracer model calculations, and which is presented in this paper.

2.1. Tropospheric NO_2 columns from GOME

The Global Ozone Monitoring Experiment (GOME) (Burrows et al., 1999) is a UV/visible spectrometer operating on the ERS-2 satellite since July 1995. GOME observes the solar radiance scattered in the atmosphere and reflected from the surface in near nadir viewing geometry. Once per day, it also takes an irradiance measurement of the sun providing an absorption free background spectrum. The instrument covers the spectral range from 240 to 790 nm in 4096 spectral channels at a resolution of 0.2–0.4 nm. The ERS-2 satellite is in a sun-synchronous near polar orbit with an equator crossing-time of 10:30. As a result, measurements at a given latitude are always at the same local time. The GOME instrument scans across the track from east to west taking three measurements of 320×40 km^2 through its swath of 960 km. With this scan

ACPD
3, 2101–2141, 2003

pattern, global coverage is achieved in three days at the equator and in one day at 65°.

From the nadir measurements and the irradiance background, integrated columns can be retrieved for a number of atmospheric trace species including O_3, NO_2, BrO, SO_2, HCHO, and H_2O (Burrows et al., 1999) using the well known Differential Optical Absorption Spectroscopy (DOAS) method (Platt, 1994). Briefly, absorbers are identified by the "fingerprint" of the wavelength dependence of their absorption structures, and the total amount of the absorber along the line of sight is determined using Lambert-Beer's law. In a second step, this column is converted to a vertical column using airmass factors (Solomon et al., 1987) derived with a radiative transport model (Rozanov et al., 1997). Since, under clear sky conditions, a fraction of the radiation received by GOME (in particular in the visible part of the spectrum) is sunlight reflected by the surface, which travelled through the entire atmosphere, GOME measurements are sensitive to both stratospheric and tropospheric absorptions. If only the tropospheric column is of interest, the stratospheric contribution to the signal has to be corrected for, which in the case of NO_2 is usually done by subtracting measurements taken on the same day at the same latitude over a clean region (Leue et al. 2001; Richter and Burrows 2002; Martin et al. 2002). This approach is based on the assumptions that a) stratospheric NO_2 does not depend on longitude, and that b) the reference region has a negligible tropospheric NO_2 burden. Tropospheric NO_2 columns from GOME have been validated against independent measurements (Heland et al., 2002), and have been extensively compared to model results (Velders et al. 2001; Lauer et al. 2002; Martin et al. 2002).

The accuracy of tropospheric NO_2 columns from GOME is mainly limited by problems associated with cloud contamination, errors introduced by the correction of the stratospheric contribution, and uncertainties in the airmass factor (Richter and Burrows, 2002). In the case study discussed here, most of the relevant scenes were cloud free (see Fig. 8), simplifying the data analysis. However, the shape of the vertical distribution of NO_2 has to be taken into account for the airmass factor calculation. In the standard analysis it is assumed that the bulk of the NO_2 is situated in the ABL.

ACPD
3, 2101–2141, 2003

In the present case, however, NO_2 was transported to the free troposphere, where the retrieval is more sensitive to NO_2. Therefore, the standard airmass factors were used only for the source regions over the continents, whereas over the ocean it was assumed that the bulk of the NO_2 was situated between 3 and 5 km, as indicated by the transport model results presented in section 3. By this approach the NO_2 vertical columns were reduced by roughly a factor of 2 over the ocean compared to the standard scientific tropospheric NO_2 GOME product, upon which the initial discovery of this event was based. The discovery, thus, did benefit from an overestimate of the NO_2 vertical columns over the ocean in the standard product, which overemphasized the ICT. However, as the overall patterns were quite similar in both analyses, only the results obtained with the modified, more realistic, airmass factors yielding reduced NO_2 columns are presented here.

Since no correction is applied for thin clouds that may have been present in the GOME pixels, the amount of NO_2 is probably underestimated, as detailed in Velders et al. (2001) and Richter and Burrows (2002). Even a cloud fraction of 10% can lead to an underestimation (overestimation) of up to 100% (50%) in the GOME measurements if the cloud is above (below) the NO2 layer. Therefore, GOME pixels with large cloud fractions (>50%) were excluded from the analysis.

When comparing GOME measurements and model results, it is also important to keep in mind that GOME can only observe NO_2, not NO_x. Depending on altitude, temperature, albedo and cloud coverage, the NO_2/NO_x ratio varies significantly in the troposphere, with most of the NO_x being in the form of NO_2 close to the surface and the significance of NO increasing with altitude. Therefore, for a given NO_x vertical column, the NO_2 column is smaller when the NO_x is located at higher altitudes. For the high solar zenith angles encountered during this study and at temperatures typical for the mid-troposphere, both NO and NO_2 contribute approximately 50% of the NO_x.

ACPD
3, 2101–2141, 2003

2.2. Model simulations

To simulate the transport, the Lagrangian particle dispersion model FLEXPART (version 4.4) (Stohl et al. 1998; Stohl and Thomson 1999; http://www.forst.tu-muenchen.de/EXT/LST/METEO/stohl/) was used. FLEXPART was validated with data from three large-scale tracer experiments in North America and Europe (Stohl et al., 1998), and it was used previously for case studies (Stohl and Trickl 1999; Forster et al. 2001; Spichtinger et al. 2001) and a 1-year "climatology" (Stohl et al., 2002a) of ICT.

For this study, FLEXPART was used with global data from the European Centre for Medium-Range Weather Forecasts (ECMWF, 1995) with a horizontal resolution of 1°, 60 vertical levels and a time resolution of 3 h (analyses at 00:00, 06:00, 12:00, 18:00 UTC; 3-h forecasts at 03:00, 09:00, 15:00, 21:00 UTC). Data with 0.5°resolution covering the domain 120° W to 30° E and 18° N to 66° N were nested into the global data in order to achieve higher resolution over the region of main interest, i.e., North America, the North Atlantic, and Europe.

FLEXPART treats advection and turbulent diffusion by calculating the trajectories of a multitude of particles. Stochastic fluctuations, obtained by solving Langevin equations (Stohl and Thomson, 1999), are superimposed on the grid-scale winds to represent transport by turbulent eddies, which are not resolved in the ECMWF data. The ECMWF data also do not resolve individual deep convective cells, although they reproduce the large-scale effects of convection (e.g. the strong ascent within WCBs). To account for sub-gridscale convective transport, FLEXPART was recently equipped with the convection scheme developed by Emanuel and Živković-Rothman (1999), as described in Seibert et al. (2001).

With FLEXPART the transport of a passive tracer was calculated, representing NO_x emissions from North America, taken from the EDGAR version 3.2 inventory (Olivier and Berdowski, 2001) (base year 1995, 1°resolution). The simulation started on 28 October and ended on 28 November 2001. During this period, a total of 25 million particles were released between the surface and 150 m above the ground at a constant

ACPD
3, 2101–2141, 2003

rate, with the number of particles released in a particular grid cell being proportional to the emissions in that cell. An exponential decay with a time constant of two days was assumed for the NO_x tracer. This is longer than the typical NO_x lifetime in the ABL, but of the right order of magnitude for NO_x transport in the free troposphere. The episode of interest started on 8 November 2001, allowing a sufficiently long model spin-up of 11 days. The simulations were described in more detail by Stohl et al. (2003).

3. A case study

3.1. Meteorological overview

The "express highway" in which pollution was carried rapidly from North America to Europe was created in a series of dynamical developments, which are described in this section. The most important ingredient to this episode was a bomb, which exploded on 7 November. This bomb itself had three precursor systems: First, a tropical depression started to develop in the Caribbean on 29 October and intensified to a category four hurricane until 4 November. In a GOES-East infrared satellite image on 3 November at 06:00 UTC, an eye can be seen clearly in the center of the hurricane (Fig. 1). This hurricane occurred unusually late in the season, but nevertheless was one of the strongest of the year. When it made landfall in Cuba on 4 November, wind speeds of up to 65 m s^{-1} caused massive destruction.

On 6 November at 00:00 UTC, the hurricane can still be seen as a minimum in the sea-level pressure, a map of which is shown in Fig. 2a, where the hurricane's position is marked with "Hu". Subsequently, the hurricane weakened, but continued heading north, carrying warm and moist tropical air with it. On 6 November at 18:00 UTC (Fig. 2b) it merged with the second bomb precursor, a cut-off low at 500 hPa (labeled "C0") that had been almost stationary over the eastern seaboard of Canada since 5 November (see Fig. 2a). Cut-off low "C0" blocked continental outflow from the northern parts of the U.S. and Canada from 5 to 8 November.

The third precursor was an extratropical moving cyclone ("C1") that formed northwest of the Hudson Bay on 5 November. On 6 November at 00:00 UTC, "C1" was located northwest of the Hudson Bay (Fig. 2a), but reached it 18 h later (Fig. 2b). "C1" connected to the cut-off cyclone "C0" on 7 November, and finally merged with it on 8 November (Fig. 2c-d). The mergers of both the hurricane "Hu" approaching from the south and the mobile cyclone "C1" approaching from the northwest with the cut-off cyclone "C0" in the middle, created an environment for explosive development, generating bomb "B1" on 8 November at 00:00 UTC (Fig. 2c).

On 8 November at 18:00 UTC, "B1" was centered west of Greenland (Fig. 2d). A combined GOES-East and METEOSAT infrared satellite image for 8 November at 18:00 UTC (Fig. 3) documents the result of this explosive cyclogenesis. It shows a truly giant bomb whose cold frontal cloud band extended from Greenland all the way into the Caribbean, and whose cloud head stretched from northern Greenland to Iceland. The total dimension of the cloud system was greater than 7000 km.

One day later (Fig. 2e), the bomb split into two ("B1" and "B2") over Greenland. While the northern center "B1" weakened, the southern center "B2" intensified, because of cyclogenesis leewards of Greenland. On 10 November at 12:00 UTC (Fig. 2f), "B2" was centered northeast of Iceland and had deepened to its minimum central sea-level pressure of 948 hPa. 18 h later, on 11 November at 06:00 UTC (not shown), "B2" travelled into Scandinavia and subsequently into Siberia, where its core pressure finally started to increase. Due to the remoteness of northern Scandinavia, the severe weather did not cause major damage, but heavy snowfalls in the mountains and a wind speed of 43 m s^{-1} were reported in Lapland on 10 November. It is furthermore to be noted that the bomb likely had triggered downstream Rossby wave breaking, thus indirectly causing the catastrophic flooding that occurred over Algeria on 10 and 11 November and caused the death of almost thousand people.

In order to confirm the classification of this system as a bomb, Fig. 4 shows the development of the bomb's minimum sea-level pressure from 5 to 12 November. At any time, the minimum sea-level pressure was taken from the core of the deepest of

the four systems, “Hu”, “C0”, “B1”, and “B2”, respectively (compare Fig. 2). During the 30-h period from 6 November 18:00 UTC to 8 November 00:00 UTC, the bomb’s core pressure decreased from about 995 hPa (in the center of the remnant of “Hu”) to 961 hPa. This pressure drop of 34 hPa/30 h clearly exceeds the criterion (21 hPa/24 h at 50° N) defined in SG1980 for explosive cyclogenesis. The bomb criterion was also met according to the 6-hourly Aviation (AVN) model analyses, obtained from the National Center for Enviromental Prediction (NCEP), where the system’s central pressure fell from about 997 hPa to 964 hPa during the same time period. The pressure rise on 9 November and the subsequent further drop on 10 November (Fig. 4) are associated with the lysis of “B1” and the genesis of “B2”. If pressure were not taken from the center of “B1”, “B2” itself would have been classified as a bomb. However, the two systems are not truly independent, as the strong zonal flow generated by “B1” over southern Greenland facilitated the lee cyclogenesis of “B2”. Therefore, and for the sake of simplicity, “B1” and “B2” are referred to here as a single bomb.

As will be seen later, the strong zonal flow south of the bomb’s center on 9 (Fig. 2e) and 10 (Fig. 2f) November was responsible for the extremely rapid transport of pollution from North America to Europe. Thus, the bomb created an “express highway” for the pollution, visualized by the dense contour lines of both sea-level pressure and 500 hPa geopotential (Fig. 2e-f). It is also important that the bomb itself travelled rapidly to the east, such that the highway was “rolled out”, like a carpet, in front of the pollution plume, and was “rolled in” after the plume’s passage, enabling rapid transport across the entire Atlantic, even though the highway did not stretch across the entire Atlantic at any particular time. However, the initial export of the pollution from the ABL over North America and its injection into the highway occurred through another system over the Great Lakes region, upstream of the bomb.

During the days preceding the NO_x export, eastern North America was under the influence of an anticyclone, which extended from Mexico north to the Hudson Bay. The anticyclone weakened on 5 November, but can still be seen in the pressure charts for 6 November at 00:00 UTC (Fig. 2a) and 18:00 UTC (Fig. 2b), where it is labeled “A”.

Upstream of the bomb "B1", yet another, much weaker, cyclonic system "C2" formed after the retreat of anticyclone "A". On 8 November 00:00 UTC (Fig. 2c), this system appears as a weak minimum west of the Great Lakes on the surface pressure analysis. 18 h later (Fig. 2d), "C2" had crossed the Great Lakes and had intensified. The cold frontal cloud band associated with "C2" extended from the Central United States to northeast of the Great Lakes (see Fig. 3), and a sequence of radar images shows a squall line progressing east. Trajectories started at 500 m above ground level southwest of the Great Lakes on 8 November 00:00 UTC ascended into the higher-level clouds northeast of the Great Lakes at 18:00 UTC (not shown). This indicates northward and upward transport of air from the ABL into the express highway that was just "rolled out" south of the bomb on 8 November at 18:00 UTC (Fig. 2d).

3.2. NO_x transport in the bomb

Fig. 5 shows daily tropospheric vertical columns of NO_2 during the period 7–11 November, obtained from GOME spectral data. Figure 6 shows corresponding atmospheric vertical columns of the FLEXPART NO_x tracer (furtheron referred to as NO_x for the sake of simplicity) during the period 7-11 November, and Fig. 7 shows meridionally oriented vertical sections through the NO_x field. The daily plots of the model results are shown for times that, in the region of main interest, coincide best with the GOME overpasses at about 10:30 local time.

On 7 November, the FLEXPART model results indicate that pollution outflow from North America was restricted to the region south of the bomb (Fig. 6a). Over the continent, the NO_x was capped at about 2 km by the subsidence inversion of the retreating anticyclone "A" (Fig. 7a). Over North America and downwind of it, the GOME tropospheric NO_2 vertical columns (Fig. 5a) show a distribution very similar to the FLEXPART results. In particular, no high values are seen over the ocean, except for a region south of the bomb and close to the continent, where pollution outflow took place. However, this outflow did not reach Europe subsequently and is not discussed further here. Thus, the situation on 7 November can be considered as typical, similar to the

ACPD
3, 2101–2141, 2003

NO_2 distributions seen in annually averaged GOME results (Leue et al. 2001; Martin et al. 2002; Richter and Burrows 2002). In contrast to GOME NO_2, the model NO_x shows no enhanced values over Europe, because only North American NO_x was simulated. Maximum GOME NO_2 values over North America are on the order of 10^{16} molecules cm^{-2} (off the scale in Fig. 5a), somewhat less but on a similar order of magnitude as the FLEXPART NO_x columns over North America. The overprediction is expected, because FLEXPART simulates the sum of NO plus NO_2, and because the assumed lifetime of 2 days is too long for conditions in the ABL.

On 8 November, the cyclone "C2" had intensified (Fig. 2d) and a NO_x plume ascended slantwise with the cyclone's WCB northeast of the Great Lakes (Fig. 7b). Note that, at this time, the NO_x was contained in the WCB clouds (compare Fig. 6b with Fig. 3). Therefore, and because ERS-2 did not overpass the entire critical region over the Great Lakes, GOME observes little of the NO_2 transport (Fig. 5b) on 8 November.

On 9 November, a filament of enhanced NO_x left North America, with the leading edge of the filament south of Greenland at 15:00 UTC (Fig. 6c). The corresponding vertical section (Fig. 7c) shows that the main part of the NO_x plume was located between about 4 and 6 km. At that time, the plume's leading edge had already emerged from the WCB (corresponding satellite images show clouds dissolving in this region), thus giving GOME the first clear opportunity to monitor the NO_x export from North America. As shown in Fig. 5c, GOME sees a maximum (about 3×10^{15} molecules cm^{-2}) northeast of Newfoundland, relatively far from any significant source of NO_x, but exactly where FLEXPART suggested pollution injection into the express highway (Fig. 6c).

On 10 November, both GOME (Fig. 5d) and FLEXPART (Fig. 6d) show a filament of enhanced NO_2 and NO_x, respectively, stretching from Newfoundland across the Atlantic almost to Scandinavia. According to FLEXPART, the leading tip of the NO_x filament had travelled from south of Greenland to Scandinavia, more than 50° of longitude (or almost 3000 km at 60° N) in only 20 h, equivalent to average wind speeds above 40 m s^{-1}. Age spectra of the NO_x (see Stohl et al., 2003, for an explanation how age spectra were obtained from FLEXPART) suggest that most of the NO_x in the leading

ACPD
3, 2101–2141, 2003

part of the filament northeast of Great Britain was emitted in North America 2-3 days before, but a significant fraction was even younger than 2 days.

Meridional cross-sections through the FLEXPART output show that the filament was located at altitudes of 4-6 km at 40° W (Fig. 7d) and 2–4 km at 10° W (Fig. 7e). The plume, thus, descended from its higher altitude on the previous day (compare with Fig. 7c). Due to the descent clouds evaporated, exposing the plume to the GOME instrument. An infrared satellite image (Fig. 8) confirms that clouds were thin or absent at the plume's location.

The highest NO_2 values observed by GOME in the filament between Iceland and Scotland were 2.5×10^{15} molecules cm^{-2}, likely a lower estimate because of partial cloudiness. Assuming that the filament's vertical extension was 2 km (Fig. 7e), simple arithmetics yields an average concentration of 1.0 $\mu g\, m^{-3}$ NO_2, corresponding to almost 1 ppbv at about 4 km altitude, within the plume. Assuming that NO contributes 50% to the NO_x, average NO_x concentrations in the plume can be estimated at nearly 2 ppbv, in good agreement with the NO_x mixing ratios obtained from the model simulation (Fig. 7e). These are very high NO_x mixing ratios in the free troposphere, which, given sufficient supply with hydrocarbons (which are likely strongly enhanced in the plume, too) and sunlight, can lead to considerable O_3 production.

On 11 November, the main part of the FLEXPART filament extended from southern Greenland to Russia (Fig. 6e). The maximum vertical columns were lower than before, both because of the further decay of the NO_x, and because the filament broadened, due to mixing with ambient air. Nevertheless, GOME was still able to see the NO_2 signal, showing a band of enhanced NO_2 values between Greenland and the Baltic Sea (Fig. 5e). The maximum within the band was detected over the Baltic Sea, at the same location where FLEXPART suggested the NO_x maximum. The cross-sections through the FLEXPART output (Fig. 7f) indicates that the vertical extension of the NO_x plume had increased considerably. In the simulation, some of the NO_x even touched down to the Baltic Sea surface.

ACPD
3, 2101–2141, 2003

3.3. Confirmation of the anthropogenic origin of the NO_x

Many previous studies (e.g. Brunner et al. 1998; Wenig et al. 2002) had difficulties with the unambiguous attribution of observed upper tropospheric NO_x plumes to anthropogenic surface emissions, because the uplift of anthropogenic pollution was associated with strong lightning activity, which can produce additional NO_x (e.g. Jeker et al., 2000). In this case, too, the vertical transport in cyclone "C2" occurred in precipitating clouds, where lightning is possible. However, this episode occurred late in the year, when lightning activity is close to its minimum in the middle latitudes. In order to reliably exclude lightning as the source of the observed NO_x, access was obtained to the lightning data from the Canadian Lightning Detection Network and the U.S. National Lightning Detection Network (NLDN) (Cummins et al., 1998). These networks detect electromagnetic signals from cloud-to-ground (CG) lightning discharges. The flash detection efficiency is about 80–90% over the continent (Cummins et al., 1998), but decreases with distance from the coast over the sea. Flash locations and times were obtained from the U.S. NLDN for the region north of 40° N and east of 100° W, covering the region where the NO_x was injected into the express highway, for the period 7-10 November 2001. Furthermore, a summary image showing all lightning flashes detected by both the Canadian and the U.S. networks was received (T. Turner, personal communication).

Few lightning flashes were detected over Canada, but a lightning episode was observed over the U.S., and another one off the coast of North America (Fig. 9). During the first episode, from 7 November 12:00 UTC to 8 November 12:00 UTC, 807 lightning flashes were detected in the Great Lakes region, which were associated with a line of isolated convective cells seen in a corresponding satellite image. The second lightning episode occurred off the coast of North America on 9 and 10 November, when 4097 lightning flashes were detected north of 40° N. Since the detection efficiency of the NLDN decreases over the sea, the number of flashes in this region may have been considerably underestimated. Furthermore, no data south of 40° N were available.

The data shown in Fig. 9 were used to make an upper estimate of the lightning NO_x emissions on the basis of emission factors reported in the literature. This estimate then served as an input for a FLEXPART lightning NO_x tracer simulation, in order to judge whether lightning could have contributed significantly to the NO_x plume detected by GOME or not. First it must be considered that the NLDN detects only CG lightning discharges, but no intracloud (IC) flashes. The ratio of IC/CG flashes over the Great Lakes region varies from 2 to 7 (Boccippio et al., 2001). Taking the higher value, it was assumed that 5649 and 28679 IC flashes occurred in the two lightning clusters (7 at each position of a CG flash).

Before estimating the NO_x production, the vertical distribution in the cloud of the lightning NO_x must be considered. Pickering et al. (1998) suggested that the downdrafts carry about 23% of the total NO_x produced from lightning, which results mostly from CG flashes, while updrafts carry 77% of the NO_x, produced by both IC and CG flashes. Here it is assumed that downdrafts released the NO_x between the surface and 1 km above, while updrafts released it between 6 and 10 km, the approximate altitude of the highest cloud tops according to satellite infrared imagery.

Values reported in the literature for the NO_x produced per cloud-to-ground lightning flash vary considerably, for instance 6.7×10^{26} molecules flash^{-1} (Price et al., 1997), 1.25-12.5$\times10^{25}$ molecules flash^{-1} (Stith et al., 1999), or 8.1×10^{25} molecules flash^{-1} (Huntrieser et al., 2002). DeCaria et al. (2000) estimated that 3×10^{26} molecules CG-flash^{-1} are carried by the downdrafts. Taking this last value, which is at the upper range of the more recent values reported in the literature, and assuming a 80% detection efficiency of CG flashes (note that this value may be too low for the second episode), it is estimated that 23.3 t (118 t) NO_2 were produced in the first (second) lightning episode below 1 km.

IC flashes produce less NO_x per flash than CG flashes (Price et al., 1997). DeCaria et al. (2000) estimate that 1.4×10^{26} molecules IC-flash^{-1} and 3×10^{26} molecules CG-flash^{-1} are carried in updrafts. Adopting these values results in a NO_2 release between 6 and 10 km of 98 t (497 t) NO_2 for the first (second) episode, if again 80% detection

ACPD
3, 2101–2141, 2003

efficiency for CG flashes is assumed.

These values can be compared to emissions of 49,000 t NO_2 per day in the entire U.S., and 880 t NO_2 per day in a single 1° ×1° grid cell over Chicago, according to the EDGAR inventory (Olivier and Berdowski, 2001). Thus, both lightning episodes seem to be negligible sources of NO_x compared to the anthropogenic source. However, as most of the lightning NO_x is transported to the anvil region, where the NO_x lifetimes are longer than in the ABL, a much larger fraction than of the anthropogenic NO_x may be available to long-range transport. Therefore, two lightning NO_x tracers were simulated with FLEXPART, one for each of the two episodes, assuming a NO_x lifetime of 2 days.

Fig. 10 shows, for both lightning clusters, the total vertical columns of the lightning NO_x tracer at the time of the GOME observations on 10 November. It is seen that a part of the NO_x produced by the first lightning cluster indeed travelled in the express highway (Fig. 10a), approximately where GOME detected the NO_2 filament. However, the maximum vertical columns in this region were only about 5×10^{12} molecules cm^{-2}, or more than two orders of magnitude less than the observed NO_2. Most of the lightning NO_x (it can be shown that it was the part released in the anvil) was located over the central North Atlantic, but even there NO_x columns were too low to be detectable by GOME.

The maximum NO_x columns resulting from the second lightning cluster (Fig. 10b) were much higher than those from the first one, but on 10 November the plume was still quite close to where it had been produced. Part of this plume was injected into the express highway and travelled to Europe subsequently, but too late to explain more than the trailing end of the GOME filament observed on 11 November. Therefore, lightning NO_x emissions from the second cluster also cannot explain the GOME observations, especially not on 10 November. Unfortunately, in this case, the NLDN may have missed lightning further off-shore, because of the decrease in detection efficiency with distance from the coast. Furthermore, no lightning data were available south of 40° N. Therefore, we repeated the FLEXPART simulations two times, first shifting the emissions 5° to the east and, second, 5° to the south. Neither of these sensitivity simu-

lations could explain the GOME observations. Therefore, lightning can be ruled out as the main source of the NO_2 detected by GOME.

4. Discussion and climatological considerations

In this paper it was shown, unambiguously for the first time, that NO_x from anthropogenic sources can be transported over intercontinental distances. More than 1 ppbv NO_x arrived over Europe within the North American plume, bearing significant capacity for O_3 formation. The key transport mechanism in this episode, strong zonal flow south of the center of a meteorological bomb, was quite exceptional and has not yet been studied in the context of atmospheric chemistry. The question, thus, arises, whether this was just an interesting event at the very extreme end of the spectrum of all transport events, or whether similar episodes do indeed happen more often. In other words: What is the climatological relevance of air pollution transport in bombs?

It is not straightforward to use GOME data for answering this question, because normally the upward transport of pollution is accompanied by extensive cloud formation, shielding NO_2 from the satellite's view. In the case presented here the clouds dissolved quickly after their formation, but this is likely not a typical situation. Furthermore, the longer lifetime of NO_x in winter than in summer favored the long-range transport of NO_x in this case. In addition, lightning may sometimes contribute a large fraction of the NO_x (at least in summer), rendering difficult the attribution of the detected NO_x to an anthropogenic source.

An answer to the above question can be given on the basis of bomb climatologies. SG1980 identified 109 and 158 bombs in the North Atlantic and North Pacific in three winter half years (maximum frequency in January), respectively, but they note that, for several reasons, bombs are underreported in their study. Similar frequencies were also reported by Roebber (2002) for another 1-year period. Using somewhat stronger criteria for bomb classification, Lim and Simmonds (2002) found 46 and 26 bomb events per year in the Northern and Southern Hemisphere, respectively. However, they only

ACPD
3, 2101–2141, 2003

considered explosive developments starting at 00:00 UTC, thus underestimating true bomb frequencies. Furthermore, all three studies used coarse-resolution meteorological data, where not all bombs could be detected. Therefore, on a global scale bombs are quite frequent phenomena. On average, a bomb event occurs about once a week on the Northern Hemisphere, and this frequency increases to one event every two days at the peak of the winter-time bomb season.

Both SG1980 and Lim and Simmonds (2002) found the highest bomb frequencies over the warm Kuroshio current and Gulf stream east of Asia and North America, respectively (see Fig. 3 in SG1980 and Fig. 12 in Lim and Simmonds (2002)), but detected few bombs over land. For the Southern Hemisphere, Lim and Simmonds (2002) report the highest bomb frequencies at about 60° S, relatively remote from pollution sources (albeit secondary maxima were detected downwind of South America and Australia). Taking this together with the lower overall bomb frequency, it seems that bombs are not a particularly relevant factor for air pollution transport on the Southern Hemisphere. On the Northern Hemisphere, however, bombs may influence transport of Asian and North American pollution to a significant extent. In contrast, bombs are negligible for transport of European pollution.

Another way to estimate the climatological relevance of bombs is to look at the frequency of express highways in transport climatologies. While fast transport is not necessarily associated with bombs only, it can be argued that a large fraction of the fastest intercontinental transport events is associated either with bombs or at least with cyclones that, albeit not quite fulfilling the bomb criterion of rapid deepening, are of extreme intensity. Note, though, that fast transport in the upper troposphere can also occur with a jet streak without involving a bomb. Therefore, in order to avoid ambiguities, the original question posed at the beginning of this discussion can be changed to: What is the climatological relevance of air pollution transport in intercontinental express highways?

Stohl et al. (2002a) presented a 1-year climatology of the pathways and timescales of ICT, which has been extended recently by Eckhardt et al. (2003) to a 15-year period,

and which is used here to answer the above question. For the climatology, FLEXPART was used to calculate the global transport of six passive continental tracers. Tracer particles were released over the continents according to the emission distribution of carbon monoxide continuously throughout the entire 15-year simulation. Particles were advected for 50 days, after which they were removed from the simulations. The model output was organized in 12 age classes (denoting time after emission), the first three ones being 0-2, 2-4, and 4-6 days, and the last one being 40-50 days. An infinite tracer lifetime was used in the simulations, but tracer decay can be approximately determined for any lifetime using the discrete age class information available in the model output. For details of the transport climatology, the reader is referred to the papers of Stohl et al. (2002a) and Eckhardt et al. (2003).

Given the above age classes, a subjective definition for intercontinental express highways is that the North America tracer arrives over Europe within less than 4 days. Note that in the case study, the bulk of the NO_x would have fulfilled this criterion. For transport from Asia to North America, the greater dimension of the Pacific Ocean must be considered. Furthermore, it is not very likely for a cyclone (and presumably also not for a bomb) to track across the whole Pacific (Hoskins and Hodges, 2002). Therefore, 6 days are used as the limit for an express highway between Asia and North America.

Figure 11 shows cumulative age spectra of the concentrations of the North America tracer and of the Asia tracer, averaged over meridionally oriented vertical planes at the west coasts of the respective downwind continent (Europe for the North America tracer, North America for the Asia tracer). It can be seen that the tracer concentrations increase by orders of magnitude as transport time increases. This is a result of increasingly slow transport mechanisms being capable of delivering tracer to the downwind continent as the transport time increases. In agreement with the climatology of bombs, express highways are found to be much more important in winter than in summer. On average, express highways, as defined above, deliver about 0.16 $\mu g\,m^{-3}$ (0.14 $\mu g\,m^{-3}$) of tracer from North America to Europe (from Asia to North America) in winter, but only 0.05 $\mu g\,m^{-3}$ (0.03 $\mu g\,m^{-3}$) in summer. In contrast, in both seasons and

ACPD
3, 2101–2141, 2003

for both tracers, about 10 μg m^{-3} of tracer are delivered to the downwind continent up to a timescale of 50 days. Therefore, in winter (summer) express highways contribute only about 1-2% (3-5%o) of the tracer that is delivered within 50 days. This makes it immediately clear that express highways bear little climatological significance for trace substances with lifetimes of the order of ten days or more.

The situation is different for trace substances with a shorter lifetime. For instance, Fig. 12 shows the results if it is assumed that the tracer has a lifetime of only 1 day (note that the values reported are valid only approximately, as the tracer decay had to be estimated from the discrete age spectra). In this case, fast transport events dominate the budgets, and express highways from North America to Europe (from Asia to North America) are responsible for about 65% (75%) of the total tracer transport in winter and 44% (60%) in summer. About 2 (4) times more tracer arrives in winter than in summer.

The absolute values of the tracers delivered with express highways are relatively small, but nevertheless significant. Let us assume, for instance, that NO_x has an average lifetime of 1 day (note that it may actually be longer for bomb transport in the free troposphere) and, furthermore, the molar ratio of NO_x and carbon monoxide emissions is about 0.16, a value typical at least for the United States (EPA, 2000), but with relatively large overall uncertainty (Parrish et al., 2002). Then it can be estimated from Fig. 12a, after conversion of CO into NO_x emissions and accounting for different molar weights, that in winter on average about 2.2 ng m^{-3} NO_x arrives over Europe with express highways. Depending on the altitude of the express highways, this translates into 2–3 pptv NO_x, a very significant fraction of the 10–30 pptv required to push the photochemical regime from O_3 destruction to O_3 production (Reeves et al., 2002). Certainly, express highways are episodic events, and a mean contribution to the NO_x in the upper troposphere may not be representative for the impact on O_3 formation. However, one can easily imagine that thin filaments, such as the one found in the case study – and as they are typical for rapid transport with strong winds and correspondingly strong wind shears –, are mixed into the hemispheric background over short time scales (note that, in the case study, the model simulations actually suggested substantial dilution of the

ACPD
3, 2101–2141, 2003

tracer). Therefore, it may well be the case that air pollution express highways have a significant influence on the chemical budget of the remote Northern Hemisphere troposphere in winter. To further explore this hypothesis, simulations with chemistry transport models are required.

5. Conclusions

The conclusions from this study are as follows:

- In a case study, very good agreement between NO_x plumes simulated by the FLEXPART tracer transport model and GOME NO_2 measurements was found.
- For this case study it was shown, unambiguously for the first time, that NO_x from anthropogenic surface sources can be transported over intercontinental distances. Lightning could definitely be ruled out as the source of the NO_x.
- Within the pollution plume originating from North America, more than 1 ppb NO_x arrived over western Europe. The fact that NO_x concentrations in the ppb range can occur so far downwind from the emission source may have implications for the ozone production in remote regions of the troposphere, particularly because they may be accompanied by high concentrations of other substances, including short-lived ones such as olefines and aldehydes.
- Meteorological bombs are a, so far unexplored, transport mechanism of extremely fast long-range air pollution transport. The pathway was termed here an intercontinental express highway.
- Air pollution transport in an intercontinental express highway across the North Atlantic can take as little as one day. The time from the emission of an air pollutant at the surface in North America to its arrival over Europe can be less than two days.

ACPD
3, 2101–2141, 2003

- A 15-year transport climatology shows that intercontinental express highways are by a factor 4 more frequent in winter than in summer, in agreement with bomb climatologies.

- The climatology furthermore indicates that intercontinental express highways bear little climatological relevance for longer-lived substances (e.g. carbon monoxide), but may be important for some short-lived substances. For a substance with a lifetime of 1 day, express highways may account for about two thirds of the total ICT.

- A rough calculation suggests that express highways connecting North America with Europe enhance the average NO_x mixing ratio over Europe by about 2–3 pptv in winter.

Acknowledgements. This study was part of the projects CONTRACE and NOXTRAM, both funded by the German Federal Ministry for Education and Research within the Atmospheric Research Program 2000 (AFO 2000). ECMWF and the German Weather Service are acknowledged for permitting access to the ECMWF archives. The GOES-EAST infrared images were made available through the UNIDATA McIDAS data stream and the METEOSAT images were released by EUMETSAT, and were made available through the NASA Marshall Space Flight Center. GOME lv1-spectra have been provided by ESA through DLR-DFD-Oberpfaffenhofen. We express our gratitude to Vaisala-GAI Inc. (T. Turner and R. Zaharescu) for providing data from the U.S. National Lightning Detection Network and a figure showing lightning flashes detected by both the Canadian and the U.S. National Lightning Detection Networks.

References

Bjerknes, V.: Synoptical representation of atmospheric motions, Q. J. R. Meteorol. Soc., 36, 167–286, 1910. 2102

Boccippio, D. J., Cummins, K. L., Christian, H. J., and Goodman, S. J.: Combined satellite- and surface-based estimation of the intracloud–cloud-to-ground lightning ratio over the continental United States, Mon. Weather Rev., 129, 108–122, 2001. 2117

Bradshaw, J. Davis, D., Grodzinsky, G., Smyth, S., Newell, R., Sandholm, S., and Liu, S.: Observed distributions of nitrogen oxides in the remote free troposphere from the NASA global tropospheric experiment programs, Rev. Geophys., 38, 61–116, 2000. 2104

Browning, K. A., Hardman, M. E., Harrold, T. W., and Pardoe, C. W.: Structure of rainbands within a mid-latitude depression, Q. J. R. Meteorol. Soc., 99, 215–231, 1973. 2103

Brunner, D., Staehelin, J., and Jeker, D.: Large-scale nitrogen oxide plumes in the tropopause region and implications for ozone, Science, 282, 1305–1309, 1998. 2105, 2116

Buckley, B. W., and Leslie, L. M.: The Australian Boxing Day storm of 1998 – Synoptic description and numerical simulations, Wea. Forecasting, 15, 543–558, 2000. 2103

Burrows, J. P., Weber, M. Buchwitz, M., Rozanov, V. V., Ladstätter, A., Weißenmayer, Richter, A., DeBeek, R., Hoogen, R., Bramstedt, K., and Eichmann, K. U.: The Global Ozone Monitoring Experiment (GOME): Mission Concept and First Scientific Results, J. Atmos. Sci., 56, 151–175, 1999. 2105, 2106, 2107

Burt, S. D. and Mansfield, D. A.: The great storm of 15–16 October 1987, Weather, 43, 90–114, 1988. 2103

Carlson, T. N.: Mid-Latitude Weather Systems, American Meteorological Society, Boston, 507, 1998. 2102

Cooper, O. R., Moody, J. L., Parrish, D. D., Trainer, M., Ryerson, T. B., Holloway, J. S., Hübler, G., Fehsenfeld, F. C., and Evans, M. J.: Trace gas composition of midlatitude cyclones over the western North Atlantic Ocean: A conceptual model, J. Geophys. Res., 107, doi: 10.1029/2001JD000901, 2002. 2103

Cummins, K. L., Murphy, M. J., Bardo, E. A., Hiscox, W. L., Pyle, R. B., and Pifer, A. E.: A combined TOA/MDF technology upgrade of the U.S. National Lightning Detection Network, J. Geophys. Res., 103, 9035–9044, 1998. 2116

DeCaria, A. J., Pickering, K. E., Stenchikov, G. L., Scala, J. R., Stith, J. L, Dye, J. E., Ridley, B. A., and Laroche, P.: A cloud-scale model study of lightning-generated NO_x in an individual thunderstorm during STERAO-A, J. Geophys. Res., 105, 11 601–11 616, 2000. 2117

Eckhardt, S., Stohl, A., James, P.: The influence of the North Atlantic Oscillation on a ir pollution transport on the Northern Hemisphere, In preparation for Atmos. Chem. Phys., 2003. 2120, 2121

ECMWF: User Guide to ECMWF Products 2.1, Meteorological Bulletin M3.2, ECMWF, Reading, UK, 1995. 2109

Emanuel, K. A., and Živković-Rothman, M.: Development and evaluation of a convection

scheme for use in climate models, J. Atmos. Sci. 56, 1766–1782, 1999. 2109
EPA: National Air Quality and Emissions Trends Report, 1998, EPA Report, EPA-454/R-00-003, EPA, 2000. 2122
Forster, C., Wandinger, U., Wotawa, G., James, P., Mattis, I., Althausen, D., Simmonds, P., O'Doherty, S., Kleefeld, C., Jennings, S. G., Schneider, J., Trickl, T., Kreipl, S., Jäger, H., and Stohl, A.: Transport of boreal forest fire emissions from Canada to Europe, J. Geophys. Res., 106, 22 887–22 906, 2001. 2104, 2109
Heland, J., Schlager, H., Richter, A., and Burrows, J. P.: First comparison of tropospheric NO_2 column densities retrieved from GOME measurements and in situ aircraft profile measurements, Geophys. Res. Lett., doi:10.1029/2002GL015528, 2002. 2107
Hoskins, B. J., and Hodges, K. I.: New perspectives on the Northern Hemisphere winter storm tracks, J. Atmos. Sci. 59, 1041–1061, 2002. 2121
Huntrieser, H., Feigl, C., Schlager, H., et al.: Airborne measurements of NO_x, tracer species and small particles during the European Lightning Nitrogen Oxides Experiment, J. Geophys. Res., 107, 10.1029/2000JD000209, 2002. 2105, 2117
Huntrieser, H., Heland, J., Stohl, A., et al.: Intercontinental transport of pollution from North America to Europe: Airborne trace gas measurements over central and northern Europe, in preparation for J. Geophys. Res., 2003. 2106
Jaeglé, L., Jacob, D. J., Wang, Y., et al.: Sources and chemistry of NO_x in the upper troposphere over the United States, Geophys. Res. Lett., 25, 1705–1708, 1998. 2104
Jaffe, D., Anderson, T., Covert, D., et al.: Transport of Asian air pollution to North America, Geophys. Res. Lett., 26, 711–714, 1999. 2104
Jeker, D. P., Pfister, L., Thompson, A. M., Brunner, D., Boccippio, D., Pickering, K. E., Wernli, H., Kondo, Y., and Staehelin, J.: Measurements of nitrogen oxides at the tropopause: Attribution to convection and correlation with lightning, J. Geophys. Res., 105, 3679–3700, 2000. 2105, 2116
Lauer, A., Dameris, M., Richter, A., and Burrows, J. P.: Tropospheric NO_2 columns: a comparison between model and retrieved data from GOME measurements, Atmos. Chem. Phys., 2, 67–78, 2002. 2107
Lawrence, M., Rasch, J. P., von Kuhlmann, R., et al.: An operational global chemical weather forecast system for field campaign support: Predictions and observations of large-scale features during INDOEX, MINOS, and CONTRACE, Atmos. Chem. Phys. Discuss., 2, 1545–1597, 2003. 2106

Lemaître, Y., Protat, A., and Scialom, G.: Dynamics of a 'bomb-like' deepening secondary cyclone from airborne Doppler radar, Q. J. R. Meteorol. Soc., 125, 2797–2818, 1999. 2103
Leue, C., Wenig, M., Wagner, T., Klimm, O., Platt, U., and Jähne, B.: Quantitative analysis of NO_x emissions from Global Ozone Monitoring Experiment satellite image sequences, J. Geophys. Res., 106, 5493–5505, 2001. 2105, 2107, 2114
Lim, E.-P. and Simmonds, I.: Explosive cyclone development in the Southern Hemisphere and a comparison with Northern Hemisphere events, Mon. Wea. Rev., 130, 2188–2209, 2002. 2103, 2104, 2119, 2120
Lin, X., Trainer, M., and Liu, S. C.: On the nonlinearity of the tropospheric ozone production, J. Geophys. Res., 93, 15 879–15 888, 1988. 2104
Martin, R. V., Chance, K., Jacob, D. J., Kurosu, T. P., Spurr, R. J. D., Bucsela, E., Gleason, J. F., Palmer, P. I., Bey, I., Fiore, A. M., Li, Q., and Yantosca, R. M.: An Improved Retrieval of Tropospheric Nitrogen Dioxide from GOME , J. Geophys. Res., 107, 4437, doi:10.1029/2001JD001027, 2002. 2107, 2114
Olivier, J. G. J. and Berdowski, J. J. M.: Global emissions sources and sinks. In: Berdowski, J., Guicherit, R. and B. J. Heij (eds.), *The Climate System*, pp. 33-78. A. A. Balkema Publishers/Swets and Zeitlinger Publishers, Lisse, The Netherlands, ISBN 90 5809 255 0, 2001. 2109, 2118
Parrish, D. D., Trainer, M., Hereid, D., Williams, E. J., Olszyna, K. J., Harley, R. A., Meagher, J. F., Fehsenfeld, F. C.: Decadal change in carbon monoxide to nitrogen oxide ratio in U.S. vehicular emissions, J. Geophys. Res., 10.1029/2001JD000720, 2002. 2122
Pickering, K. E., Wang, Y., Tao, W.-K., Price, C., and Müller, J.-F.: Vertical distributions of lightning NO_x for use in regional and global chemical transport models, J. Geophys. Res., 103, 31 203–31 216, 1998. 2117
Platt, U.: Differential optical absorption spectroscopy (DOAS), in Air Monitoring by Spectroscopic Techniques, M. W. Sigrist (Ed.), Chemical Analysis Series Vol. 127, John Wiley, New York, 1994. 2107
Prados, A. I., Dickerson, R. R., Doddridge, B. G., Milne, P. A., Moody, J. L., and Merrill, J. T.: Transport of ozone and pollutants from North America to the North Atlantic Ocean during the 1996 Atmosphere/Ocean Chemistry Experiment (AEROCE) intensive, J. Geophys. Res. 104, 26 219–26 233, 1999. 2105
Price, C., Penner, J., and Prather, M.: NO_x from lightning – 1. Global distribution based on lightning physics, J. Geophys. Res. 102, 5929–5941, 1997. 2117

Reeves, C. E., Claire, E., Penkett, S. A., et al.: Potential for photochemical ozone formation in the troposphere over the North Atlantic as derived from aircraft observations during ACSOE, J. Geophys. Res., 107, 4707, doi: 10.1029/2002JD002415, 2002. 2104, 2122

Richter, A. and Burrows, J. P.: Tropospheric NO2 from GOME measurements, Adv. Space Res., 29, 1673-1683, 2002. 2107, 2108, 2114

Roebber, P. J.: Statistical analysis and updated climatology of explosive cyclones, Mon. Wea. Rev., 112, 1577–1589, 1984. 2119

Rozanov, V., Diebel, D., Spurr, R. J. D., and Burrows, J. P.: GOMETRAN: A radiative transfer model for the satellite project GOME - the plane parallel version, J. Geophys. Res., 102, 16 683–16 696, 1997. 2107

Sanders, F. and Gyakum, J. R.: Synoptic-dynamic climatology of the “bomb”, Mon. Wea. Rev., 108, 1589–1606, 1980. 2103

Seibert, P., Krüger, B., and Frank, A.: Parametrisation of convective mixing in a Lagrangian particle dispersion model, Proceedings of the 5th GLOREAM Workshop, Wengen, Switzerland, 24–26 September 2001. 2109

Solomon, S., Schmeltekopf, A. L., and Sanders, R. W.: On the interpretation of zenith sky absorption measurements, J. Geophys. Res, 92, 8311–8319, 1987. 2107

Spichtinger, N., Wenig, M., James, P., Wagner, T., Platt, U., and Stohl, A.: Satellite detection of a continental-scale plume of nitrogen oxides from boreal forest fires, Geophys. Res. Lett., 28, 4579–4582, 2001. 2105, 2109

Stith, J., Dye, J., Ridley, B., Laroche, P., Defer, E., Baumann, K., Hbler, G., Zerr, R., and Venticinque, M.: NO signatures from lightning flashes, J. Geophys. Res., 104, 16 081–16 089, 1999. 2117

Stohl, A.: A one-year Lagrangian ”climatology” of airstreams in the northern hemisphere troposphere and lowermost stratosphere, J. Geophys. Res. 106, 7263–7279, 2001. 2104

Stohl, A., Eckhardt, S., Forster, C., James, P., and Spichtinger, N.: On the pathways and timescales of intercontinental air pollution transport, J. Geophys. Res., 107, 4684, doi: 10.1029/2001JD001396, 2002a. 2109, 2120, 2121

Stohl, A., Trainer, M., Ryerson, T. B., Holloway, J. S., and Parrish, D. D.: Export of NO_y from the North American boundary layer during 1996 and 1997 North Atlantic Regional Experiments, J. Geophys. Res., 107, doi: 10.1029/2001JD000519, 2002b. 2105

Stohl, A., Hittenberger, M., and Wotawa, G.: Validation of the Lagrangian particle dispersion model FLEXPART against large scale tracer experiment data, Atmos. Environ., 32, 4245–

4264, 1998. 2109
Stohl, A. and Trickl, T.: A textbook example of long-range transport: Simultaneous observation of ozone maxima of stratospheric and North American origin in the free troposphere over Europe, J. Geophys. Res., 104, 30 445–30 462, 1999. 2103, 2104, 2109
Stohl, A. and Thomson, D. J.: A density correction for Lagrangian particle dispersion models, Boundary-Layer Meteorol., 90, 155–167, 1999. 2109
Stohl, A., Forster, C., Eckhardt, S., Spichtinger, N., Huntrieser, H., Heland, J., Schlager, H., Wilhelm, S., Arnold, F., and Cooper, O.: A backward modeling study of intercontinental pollution transport using aircraft measurements, J. Geophys. Res., in press, 2003. 2106, 2110, 2114
Ulbrich, U., Fink, A. H., Klawa, M., and Pinto, J. G.: Three extreme storms over Europe in December 1999, Weather, 56, 70–80, 2001. 2103, 2104
Velders, G. J. M., Granier, C., Portmann, R. W., Pfeilsticker, K., Wenig, M., Wagner, T., Platt, U., Richter, A., and Burrows, J. P.: Global tropospheric NO_2 column distributions: Comparing 3-D model calculations with GOME measurements, J. Geophys. Res., 106, 12 643–12 660, 2001. 2107, 2108
Wenig, M., Spichtinger, N., Stohl, A., Held, G., Beirle, S., Wagner, T., Jähne, B., and Platt, U.: Intercontinental transport of nitrogen oxide pollution plumes, Atmos. Chem. Phys. Discuss., 2, 2151–2165, 2002. 2105, 2116
Wernli, H., Dirren, S., Liniger, M. A., and Zillig, F.: Dynamical aspects of the life cycle of the winter storm 'Lothar' (24-26 December 1999), Q. J. R. Meteorol. Soc., 128, 405–429, 2002. 2103
Wild, O., Law, K. S., McKenna, D. S., et al.: Photochemical trajectory modeling studies of the North Atlantic region during August 1993, J. Geophys. Res., 101, 29 269–29 288, 1996. 2105
Zhu, Y. and Newell, R. E.: Atmospheric rivers and bombs, Geophys. Res. Lett., 21, 1999–2002, 1994. 2103
Ziereis, H., Schlager, H., Schulte, P., van Velthoven, P. F. J., and Slemr, F.: Distributions of NO, NO_x, and NO_y in the upper troposphere and lower stratosphere between 28° and 61° N during POLINAT 2, J. Geophys. Res., 105, 3653–3664, 2000. 2105

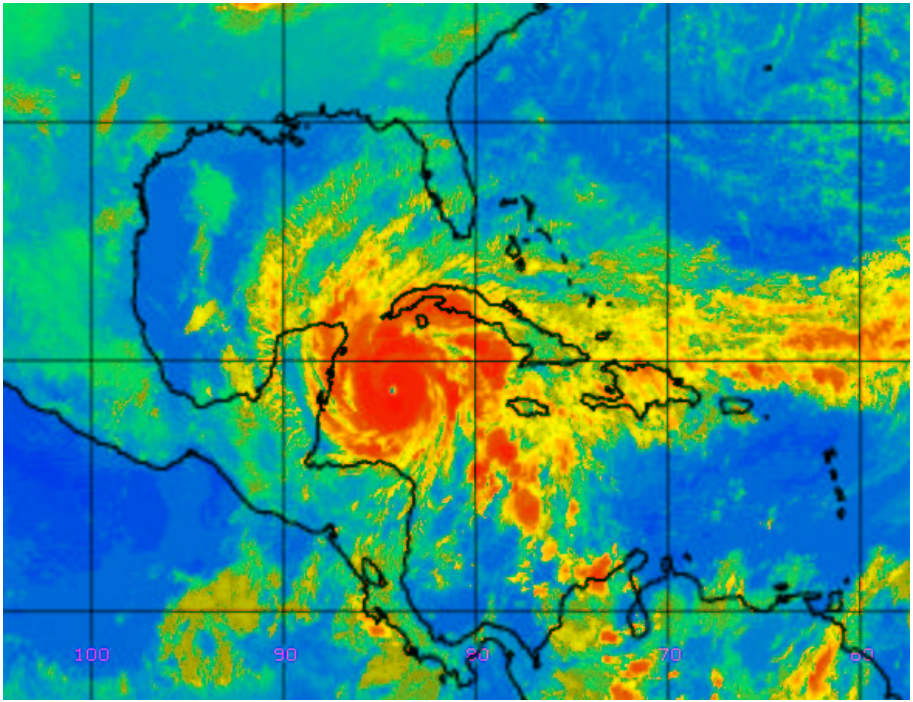

Fig. 1. GOES-East infrared satellite image of the hurricane on 3 November at 06:00 UTC.

ACPD

3, 2101–2141, 2003

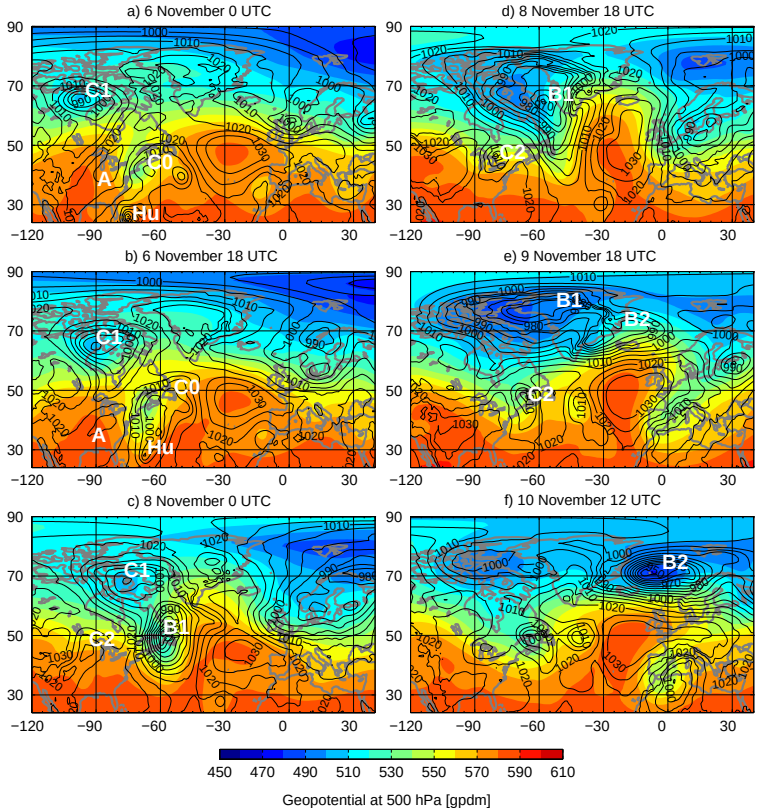

Fig. 2. Maps (120° W–40° E, 25° N–90° N) of the geopotential height at 500 hPa (color shading) and sea-level pressure (black contour lines drawn every 5 hPa) on 6 November 18:00 UTC (a), 8 November 00:00 UTC (b), 8 November 18:00 UTC (c), and 10 November 12:00 UTC (d), based on ECMWF analyses with a resolution of 1°. Continental outlines are shown as thick grey lines, and synoptic systems are labeled, as described in the text, with bold white letters northeast of their center.

ACPD
3, 2101–2141, 2003

Express highway associated with a bomb

A. Stohl et al.

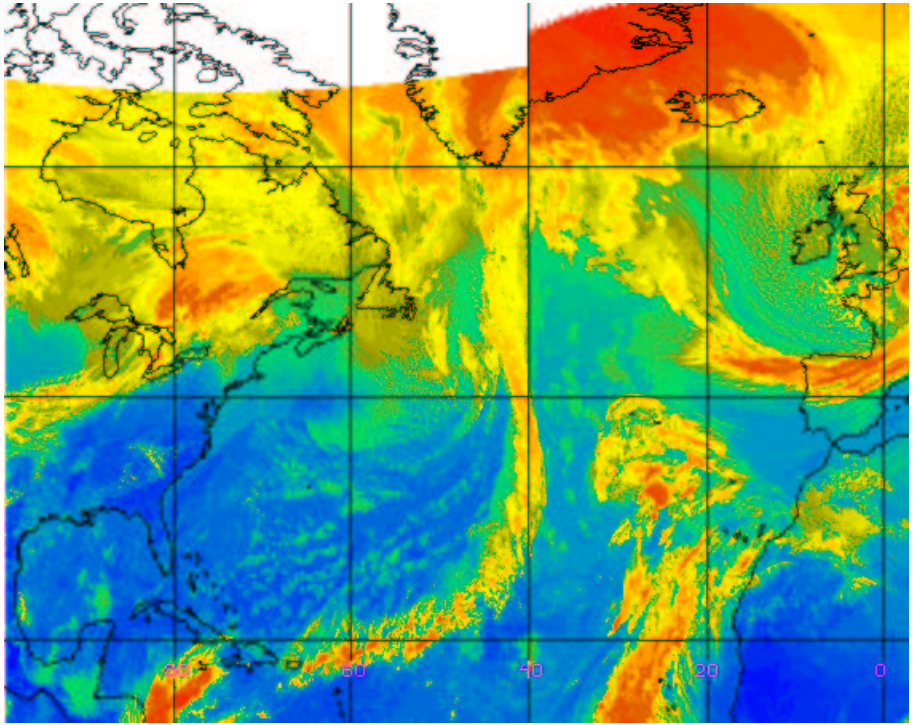

Fig. 3. Combined GOES-East and METEOSAT infrared satellite image on 8 November at 18:00 UTC. White areas in the northern part of the figure are regions without data.

ACPD

3, 2101–2141, 2003

Fig. 4. Minimum sea-level pressure from ECMWF analyses in the core of the bomb during the period 5–12 November 2001 at six-hourly intervals.

ACPD
3, 2101–2141, 2003

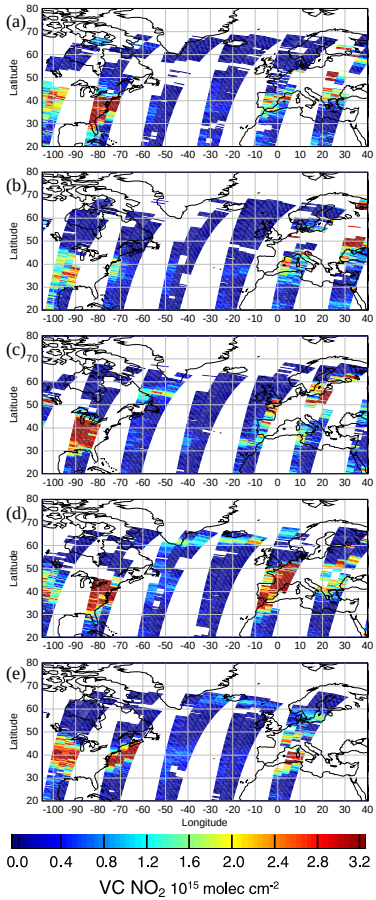

Fig. 5. Tropospheric vertical columns of NO_2 (in 10^{15} molecules cm^{-2}), retrieved from GOME spectral data on **(a)** 7, **(b)** 8, **(c)** 9, **(d)** 10, and **(e)** 11 November 2001. White regions indicate that data are missing either because no GOME overpass was available, or because of more than 50% cloud cover.

ACPD
3, 2101–2141, 2003

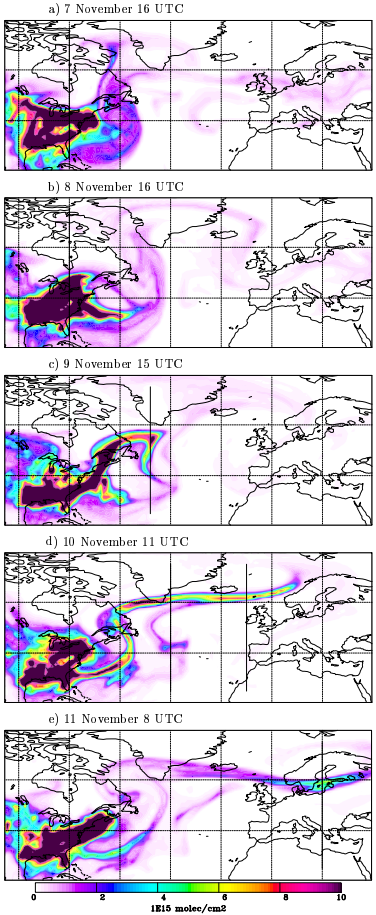

Fig. 6. Total vertical columns of the FLEXPART NO_x tracer (in 10^{15} molecules cm^{-2}) on **(a)** 7, **(b)** 8, **(c)** 9, **(d)** 10, and **(e)** 11 November. The columns are averages over 1-h periods ending at 16, 16, 15, 11, and 08:00 UTC, respectively. Bold black lines mark meridional sections shown in Fig. 7.

ACPD
3, 2101–2141, 2003

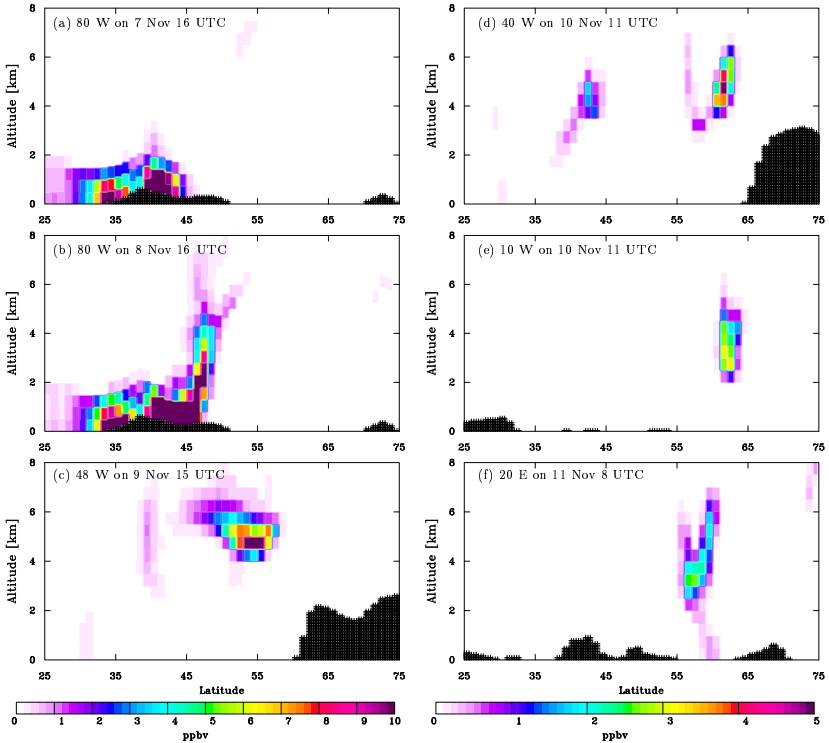

Fig. 7. Meridional cross-sections through the FLEXPART NO_x tracer (in ppbv) **(a)** along 80° W on 7 November at 16:00 UTC, **(b)** along 80° W on 8 November at 16:00 UTC, **(c)** along 48° W on 9 November at 15:00 UTC, **(d)** along 40° W on 10 November at 11:00 UTC, **(e)** along 10° W on 10 November at 11:00 UTC, **(f)** along 20° E on 11 November at 08:00 UTC. Hatched areas indicate topography. Note the difference in the NO_x scale between the left and right column of figures.

ACPD
3, 2101–2141, 2003

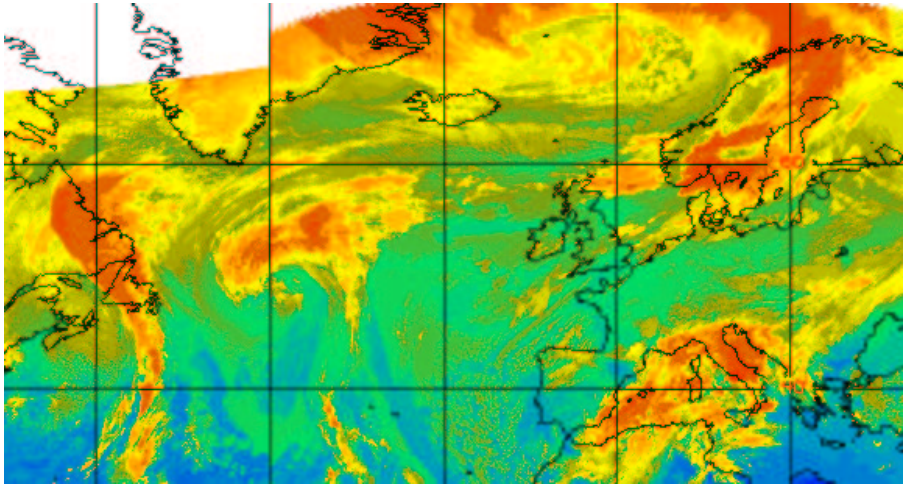

Fig. 8. Combined GOES-East and METEOSAT infrared satellite image on 10 November at 12:00 UTC. White areas in the northwest corner are regions without data.

ACPD

3, 2101–2141, 2003

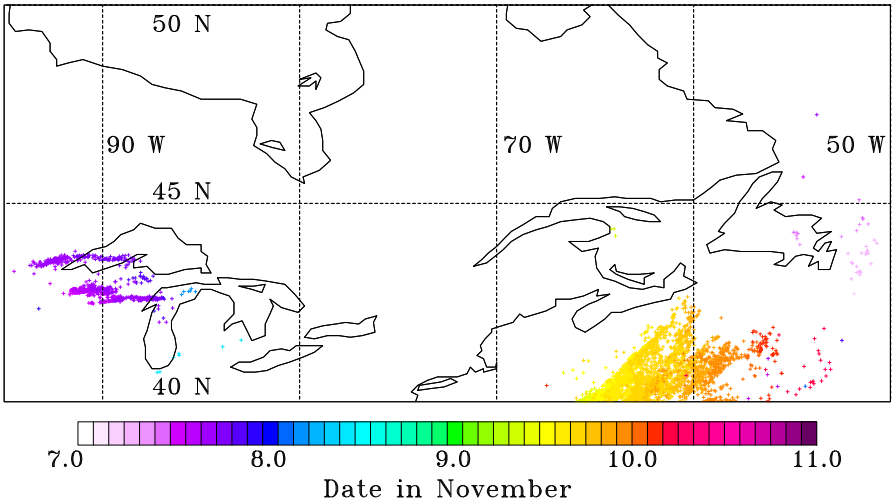

Fig. 9. Locations of lightning flashes detected by the U.S. National Lightning Detection Network during the period from 7 November 00:00 UTC to 11 November 00:00 UTC. The color of the plusses indicates the time of lightning.

ACPD
3, 2101–2141, 2003

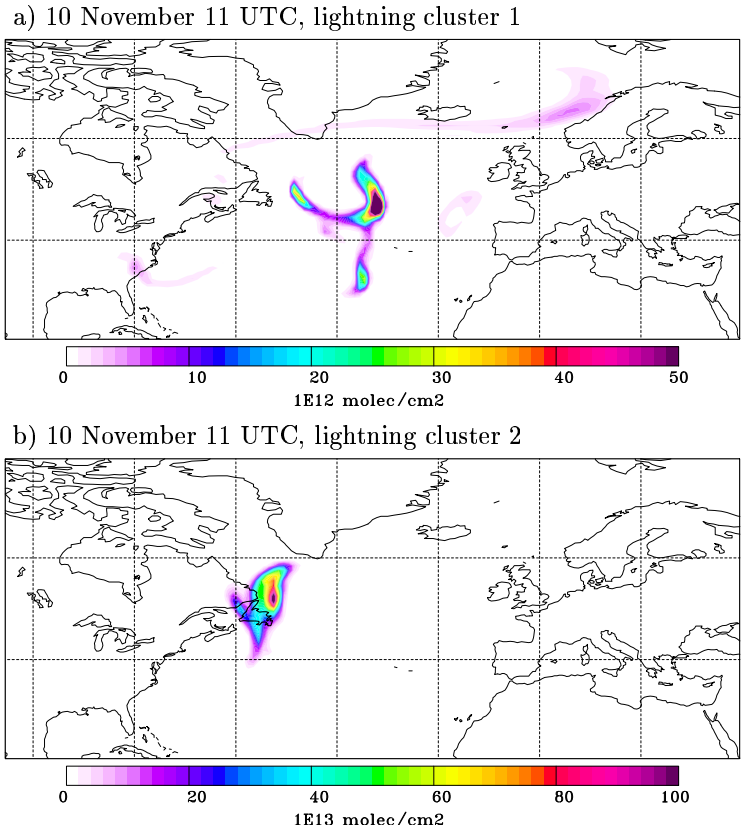

Fig. 10. Total vertical columns of the FLEXPART lightning NO_x tracer on 10 November at 11:00 UTC for (a) lightning cluster 1 (in 10^{12} molecules cm^{-2}), and (b) lightning cluster 2 (in 10^{13} molecules cm^{-2}).

ACPD
3, 2101–2141, 2003

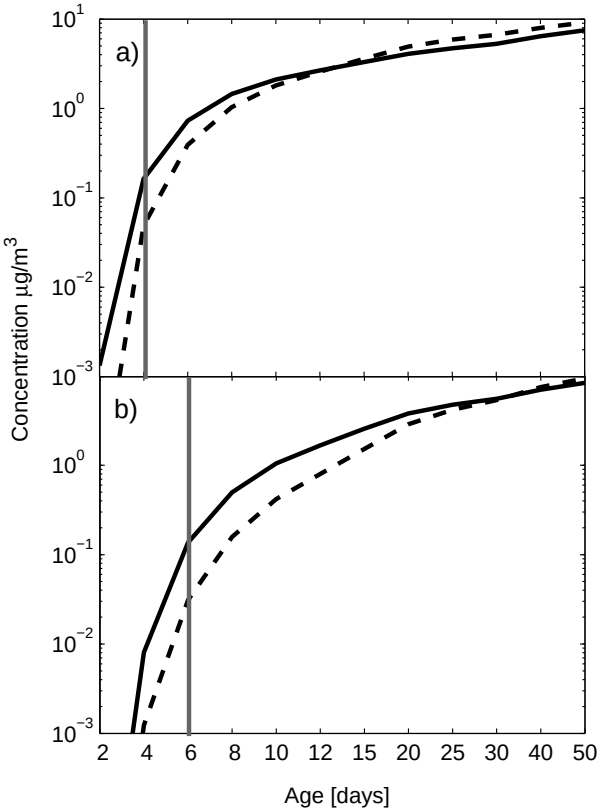

Fig. 11. Cumulative age spectra, averaged over a meridionally oriented vertical (up to 10 km) plane, in December, January and February (solid lines) and in June, July and August (dashed lines) of (a) the North America tracer at 0° W between 36° N and 70° N, and (b) the Asia tracer at 125° W between 20° N and 70° N. Values are plotted at the end of the respective age class interval. Grey vertical lines separate express highways (to the left) from slower modes of transport (to the right).

ACPD
3, 2101–2141, 2003

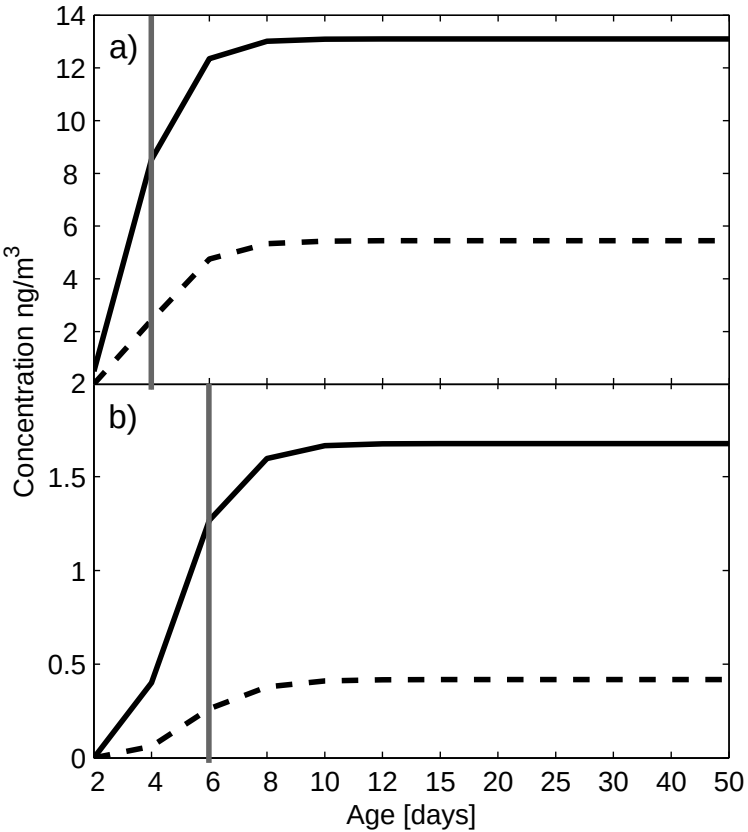

Fig. 12. Same as Fig. 11, but assuming a 1-day lifetime of the tracer. Note that a linear scale is used here, in contrast to Fig. 11.

ACPD

3, 2101–2141, 2003

Express highway associated with a bomb

A. Stohl et al.